Proceedings of the
American Control Conference
Seattle, Washington • June 1995

Design and Implementation of a Trajectory Tracking Controller for an Autonomous Underwater Vehicle (AUV) *

Carlos Silvestre† P. Oliveira† António Pascoal† D. Fryxell† Isaac Kaminer ‡

†Department of Electrical Engineering and
Institute for Systems and Robotics (ISR),
Instituto Superior Técnico,
Av. Rovisco Pais,
1096 Lisbon Codex, Portugal.

‡Department of Aeronautical
and Astronautical Engineering,
Naval Postgraduate School,
Monterey, CA 93943, USA.

Abstract

This paper proposes a new methodology for integrated design of guidance and control systems for autonomous underwater vehicles (AUVs). The methodology developed leads to a systematic procedure for the design of controllers for AUVs to accurately track reference trajectories defined in an inertial reference frame. The paper illustrates the application of this procedure to the design of a tracking controller for the AUV MARIUS. The design phase is summarized, and the performance of the resulting controller is assessed in simulation using dynamic models of the vehicle and its sensor suite.

1 Introduction. Guidance, Control and Navigation

In a great number of envisioned mission scenarios, Autonomous Underwater Vehicles (AUVs) will be required to follow inertial reference trajectories accurately [10]. To achieve that goal, the following systems must be designed and implemented on-board AUVs: i) *navigation*, to provide estimates of linear and angular positions and velocities of the vehicle, ii) *guidance*, to process navigation/inertial reference trajectory data and output set-points for the vehicle's (body) velocity and attitude, and iii) *control*, to generate the actuator signals that are required to drive the actual velocity and attitude of the vehicle to the values commanded by the guidance scheme.

Traditionally, control and guidance systems are designed separately, using well established design methods for control and simple strategies such as line of sight (LOS) for guidance, see [6] and the references therein. During the design phase, the control system is usually designed with sufficiently large bandwidth to track the commands that are expected from the guidance system. However, since the two systems are effectively coupled, stability and adequate performance of the combined system about nominal trajectories are not guaranteed. In practice, this problem can be resolved by judicious choice of guidance law parameters (such as so-called visibility distance in LOS strategy), based on extensive computer simulations. Even when stability is obtained, however, the resulting strategy leads to finite trajectory tracking errors, the magnitude of which depends on the type of trajectory to be tracked (radius of curvature, vehicle's desired speed, etc,).

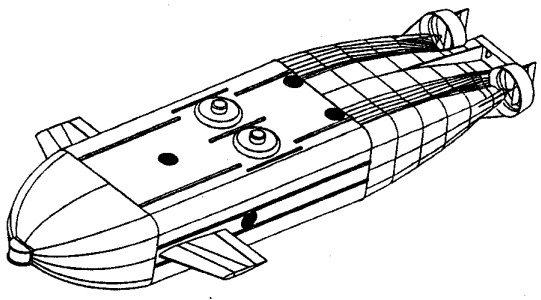

Figure 1.1: The vehicle MARIUS

This paper proposes a new methodology for the design of guidance and control systems for AUVs, whereby the two systems are effectively designed simultaneously. The key idea is to realize that for these types of vehicles the equilibrium (also known as trimming) trajectories are helices parameterized by the vehicle's body axis velocity, yaw rate and flight path angle [4]. Furthermore, using a convenient coordinate transformation, the linearization of the vehicle error dynamics and kinematics about any trimming trajectory can be shown to be time-invariant [11]. Thus, the problem of designing integrated guidance/control systems to track inertial trajectories that consist of the piecewise union of trimming trajectories, falls within the scope of gain scheduled control theory [7]. Using this approach, the vehicle's body axis velocity, yaw rate, and flight path angle play the role of scheduling variables that interpolate the parameters of linear controllers designed for a finite number of representative trimming trajectories. The results reported in [7] on so-called D-implementation of gain scheduled controllers can then be used to obtain a combined

*This work was supported by the Commission of the European Communities under contract MAS2-CT92-0021 of the the Marine Science and Technology Programme (MAST-II). The fifth author was supported by Naval Air Command under grant AIRTASK A546546TD, NSF under grant ECS-9096109, AFOSR under grant no. F49620-93-1-0246 and ARO under grant no. DAAH04-93-G-0012, and by a NATO Fellowship during his stay at IST in the Summmer of 1994.

guidance/control system such that the properties of the linear designs are recovered locally, about each trimming trajectory. This new approach guarantees that the steady state tracking error about any trimming trajectory condition is zero. Moreover, the D-implementation method leads naturally to a structure where the only exogenous commands required are the desired linear inertial position and yaw rate, thus avoiding the need to feedforward the trimming conditions for the remaining state variables. Due to space limitations, the methodology used for the design of combined guidance/control is only briefly summarized here. For complete details, see [11].

The paper is organized as follows: Section 2 introduces the model of the AUV MARIUS and derives its linearized equations of motion about trimming trajectories. Section 3 describes the structure of a gain scheduled trajectory tracking controller for the vehicle. Finally, Section 4 assesses the performance of combined guidance and control in simulation.

2 Vehicle Dynamics.

This section describes the dynamic model of the AUV MARIUS, depicted in figure 1.1. A complete study of the AUV dynamics based on hydrodynamic tank tests with a Planar Motion Mechanism (PMM) [1] can be found in [5]. In what follows, $\{I\}$ denotes a universal reference frame, and $\{B\}$ denotes a body-fixed coordinate frame that moves with the AUV. The following notation is required:

$\mathbf{p} = [x,\ y,\ z]'$ - position of the origin of $\{B\}$ expressed in $\{I\}$;

$\mathbf{v} = [u,\ v,\ w]'$ -linear velocity of the origin of $\{B\}$ relative to $\{I\}$, expressed in $\{B\}$;

$\boldsymbol{\lambda} = (\phi,\ \theta,\ \psi)'$ - vector of Euler angles which describe the orientation of frame $\{B\}$ with respect to $\{I\}$

$\boldsymbol{\omega} = [p,\ q,\ r]'$ - angular velocity of $\{B\}$ relative to $\{I\}$, expressed in $\{B\}$;

$\mathbf{R} = \mathbf{R}(\boldsymbol{\lambda})$ - rotation matrix from $\{B\}$ to $\{I\}$.

$\mathbf{Q} = \mathbf{Q}(\boldsymbol{\lambda})$ - matrix that relates $\boldsymbol{\lambda}$ to $\boldsymbol{\omega}$ and satisfies $\dot{\boldsymbol{\lambda}} = \mathbf{Q}(\boldsymbol{\lambda})\boldsymbol{\omega}$.

The symbol $\boldsymbol{\delta} := [\delta_{a,c}, \delta_{a,d}, \delta_e, \delta_r]'$ denotes the vector whose entries correspond to deflections of the ailerons (common and differential), elevator, and rudder, respectively and the symbol n denotes the propeller rotational rate. With the above notation, the dynamics of the AUV can be written in compact form as

$$M_{RB}\ddot{\mathbf{q}} + C_{RB}(\dot{\mathbf{q}})\dot{\mathbf{q}} = \boldsymbol{\tau}(\ddot{\mathbf{q}}, \dot{\mathbf{q}}, \boldsymbol{\lambda}, \boldsymbol{\delta}, n), \qquad (2.1)$$

where $\boldsymbol{\tau}$ denotes the vector of external forces, $\dot{\mathbf{q}} = [\mathbf{v}', \boldsymbol{\omega}']'$, and M_{RB} and C_{RB} denote the rigid body inertia matrix and the matrix of Coriolis and centrifugal terms, respectively. The vector $\boldsymbol{\tau}$ can further be decomposed as

$$\begin{aligned}\boldsymbol{\tau}(\ddot{\mathbf{q}}, \dot{\mathbf{q}}, \boldsymbol{\lambda}, \boldsymbol{\delta}, n) &= \boldsymbol{\tau}_{rest}(\boldsymbol{\lambda}) + \boldsymbol{\tau}_{add}(\ddot{\mathbf{q}}, \dot{\mathbf{q}}) \qquad (2.2)\\ &+\boldsymbol{\tau}_{lift}(\dot{\mathbf{q}}, \boldsymbol{\delta}) + \boldsymbol{\tau}_{visc}(\dot{\mathbf{q}}, \boldsymbol{\delta}) + \boldsymbol{\tau}_{prop}(n),\end{aligned}$$

where $\boldsymbol{\tau}_{rest}$ denotes the forces and moments caused by gravity and buoyancy and $\boldsymbol{\tau}_{add}$ is the added mass term. The term $\boldsymbol{\tau}_{lift}$ captures the effects of the lifting forces generated by the deflecting surfaces, $\boldsymbol{\tau}_{visc}$ consists of the forces and moments caused by skin friction, and $\boldsymbol{\tau}_{prop}$ represents the forces and moments generated by the main propellers. Using equation (2.1) and the associated kinematic relationships, the state space model for the AUV can be written as

$$\mathcal{G} = \begin{cases} \ddot{\mathbf{q}} &= F(\dot{\mathbf{q}}, \boldsymbol{\lambda}) \ + \ G(\dot{\mathbf{q}})H(\dot{\mathbf{q}}, \mathbf{u}) \\ \dot{\mathbf{p}} &= \mathbf{R}\,\mathbf{v} \\ \dot{\boldsymbol{\lambda}} &= \mathbf{Q}\,\boldsymbol{\omega}, \end{cases} \qquad (2.3)$$

where F, G and H are continuously differentiable functions, $\mathbf{v}$, $\boldsymbol{\omega}$, $\mathbf{p}$ and $\boldsymbol{\lambda}$ are state space variables, and $\mathbf{u} = [\boldsymbol{\delta}', n]'$ is the vector of control inputs. An equilibrium or trimming trajectory of (2.3) is defined as a path $\mathcal{P}_c = [\dot{\mathbf{q}}_C', \mathbf{p}_C', \boldsymbol{\lambda}_C']'$ such that

$$F(\dot{\mathbf{q}}_C, \boldsymbol{\lambda}_C) \ + \ G(\dot{\mathbf{q}}_C)H(\dot{\mathbf{q}}_C, \mathbf{u}_C) = 0 \qquad (2.4)$$

for some constant vector $\mathbf{u}_C$. Notice that for simplicity, the equations do not show the explicit dependence on time.

From equation (2.1), it can be concluded that the only possible trimming trajectories $\mathcal{P}_c$ correspond to helices defined by

$$\dot{\boldsymbol{\lambda}}_C = \begin{bmatrix} 0 \\ 0 \\ \dot{\psi}_C \end{bmatrix}, \quad \dot{\mathbf{p}}_C = \begin{bmatrix} \mathbf{V}_{T_C}\cos(\dot{\psi}_C t) \\ \mathbf{V}_{T_C}\sin(\dot{\psi}_C t) \\ \sin(\gamma_C) \end{bmatrix}, \qquad (2.5)$$

where $\dot{\psi}_C$ is yaw rate, $\mathbf{V}_{T_C} = ||\mathbf{v}_C||$ is body linear speed and γ_C is so-called flight path angle. Thus, the trimming trajectories can be parameterized by the vector $\alpha_c = [\mathbf{V}_{T_C}, \dot{\psi}_C, \gamma_C] \in \mathcal{R}^3$.

Given α_c, the corresponding trimming values for the state variables of (2.3) can be determined from analytical and numerical computations, as follows. Let $G^{\perp}(\dot{\mathbf{q}})$ be the orthogonal complement of $G(\dot{\mathbf{q}})$ satisfying $G^{\perp}(\dot{\mathbf{q}})G(\dot{\mathbf{q}}) = 0$. Multiplying the first equation of (2.3) by $G^{\perp}(\dot{\mathbf{q}})$, it follows that

$$\begin{cases} 0 &= G^{\perp}(\dot{\mathbf{q}}_C)F(\dot{\mathbf{q}}_C, \boldsymbol{\lambda}_C) \\ \dot{\mathbf{p}}_C &= \mathbf{R}_C\,\mathbf{v}_C \\ \dot{\boldsymbol{\lambda}}_C &= \mathbf{Q}_C\,\boldsymbol{\omega}_C \end{cases} \qquad (2.6)$$

along a trimming trajectory, thus eliminating the control input $\mathbf{u}_C$. By requiring that $\delta_{a,c} = 0$ at trimming, it can be shown that (2.6), together (2.5), provide a set of equations that can be solved numerically to give $\mathbf{v}, \boldsymbol{\omega}, \phi, \theta$ as functions of $\mathbf{V}_{T_C}, \gamma_C, \dot{\psi}_C$, thus concluding the computation of all relevant state variables at trimming. For complete details, the reader is referred to

[11]. In what follows, the symbol $\mathcal{P}_c(\alpha_c)$ denotes a path parameterized by α_c.

Let $\mathcal{P}_c(\alpha_c)$ be a trimming trajectory for the vehicle, and define the variables

$$\begin{cases} \mathbf{v}_E = \mathbf{v} - \mathbf{v}_C \\ \boldsymbol{\omega}_E = \boldsymbol{\omega} - \boldsymbol{\omega}_C \\ \mathbf{p}_E = \mathbf{R}^{-1}(\mathbf{p} - \mathbf{p}_C) \\ \boldsymbol{\lambda}_E = \mathbf{Q}^{-1}(\boldsymbol{\lambda} - \boldsymbol{\lambda}_C), \end{cases} \tag{2.7}$$

which can be interpreted as the generalized error vector between the vehicle state and the trajectory $\mathcal{P}_c(\alpha_c)$. Let $\mathbf{u}_E = \mathbf{u} - \mathbf{u}_C$. By noticing that $\mathbf{v}_C$ and $\boldsymbol{\omega}_C$ are constant along trimming trajectories, straightforward computations show that

$$\begin{cases} \ddot{\mathbf{q}}_E = \mathcal{F}(\dot{\mathbf{q}}_E, \boldsymbol{\lambda}_E) + \mathcal{G}(\dot{\mathbf{q}}_E)\mathcal{H}(\dot{\mathbf{q}}_E, \mathbf{u}_E) \\ \dot{\mathbf{p}}_E = \mathbf{v}_E + \mathbf{v}_C - \mathbf{R}_C^{-1}\mathbf{R}\,\mathbf{v}_C - S(\boldsymbol{\omega}_E + \boldsymbol{\omega}_C)\mathbf{p}_E \\ \dot{\boldsymbol{\lambda}}_E = \boldsymbol{\omega}_E + \boldsymbol{\omega}_C - \mathbf{Q}^{-1}\dot{\mathbf{Q}}_C\,\boldsymbol{\omega}_C + \dot{\mathbf{Q}}^{-1}\,\mathbf{Q}\,\boldsymbol{\lambda}_E, \end{cases} \tag{2.8}$$

where

$$\begin{aligned} \mathcal{F}(\dot{\mathbf{q}}_E, \boldsymbol{\lambda}_E) &= F(\dot{\mathbf{q}}_E + \dot{\mathbf{q}}_C, \mathbf{Q}\,\boldsymbol{\lambda}_E + \boldsymbol{\lambda}_C) \\ \mathcal{G}(\dot{\mathbf{q}}_E) &= G(\dot{\mathbf{q}}_E + \dot{\mathbf{q}}_C) \\ \mathcal{H}(\dot{\mathbf{q}}_E, \mathbf{u}) &= H(\dot{\mathbf{q}}_E + \dot{\mathbf{q}}_C, \mathbf{u}_E + \mathbf{u}_C), \end{aligned}$$

and $S(\boldsymbol{\omega})$ is the skew-symmetric matrix defined by $S(\boldsymbol{\omega}) = \boldsymbol{\omega}\times$. It is now possible to prove that the linearization of (2.8) about the error vector $[0'_{12\times 1}\mathbf{u}'_C]'$ is *time-invariant* and can be written in the form

$$\begin{cases} \delta\ddot{\mathbf{q}}_E = A_{\dot{q}_E}(\alpha_c)\delta\ddot{\mathbf{q}}_E + A_{\lambda_E}(\alpha_c)\delta\boldsymbol{\lambda}_E + B(\alpha_c)\delta\mathbf{u}_E \\ \delta\dot{\mathbf{p}}_E = \delta\mathbf{v}_E - S(\boldsymbol{\omega}_C)\delta\mathbf{p}_E - S(\mathbf{v}_C)\delta\boldsymbol{\lambda}_E \\ \delta\dot{\boldsymbol{\lambda}}_E = \delta\boldsymbol{\omega}_E - S(\boldsymbol{\omega}_C)\delta\boldsymbol{\lambda}_E \end{cases} \tag{2.9}$$

where the matrices

$$\begin{aligned} A_x &= \tfrac{\partial}{\partial x}[\mathcal{F}(x,y) + \mathcal{G}(x)\mathcal{H}(x,z)], \\ B &= \tfrac{\partial}{\partial z}[\mathcal{G}(x,y)\mathcal{H}(x,z)], \end{aligned}$$

are computed at equilibrium values. Throughout the rest of the paper, the symbol $\mathcal{G}_l(\alpha_c)$ denotes the linearized time-invariant system with realization (2.9) determined by the parameter α_c.

3 Guidance/Control System

Suppose that associated to each linearized system $\mathcal{G}_l(\alpha_c)$ there is a linear time-invariant controller $\mathcal{K}(\alpha_c)$ that stabilizes and achieves adequate performance for the closed-loop system, as evaluated by some performance criterion. Theoretically, it is then possible to define a gain-scheduled controller $\mathcal{C}$ that recruits the appropriate linear controller $\mathcal{K}(\alpha)$ based on the measured value α of the parameter α_c.

In practice, $\mathcal{C}$ is obtained by designing a family of linear controllers for a *finite* number of systems $\mathcal{G}_l(\alpha_c)$, and interpolating between these controllers to achieve adequate performance for all linearized plants in the regimes where the vehicle is expected to operate. During real time operation, the controller parameters are updated as functions of the scheduling variable $\alpha = [\mathbf{V}_T, \dot{\psi}, \gamma]'$.

3.1 Linear Controller Design

The methodology selected for linear control system design was $\mathcal{H}_\infty$ [3]. This method rests on a firm theoretical basis, and leads naturally to an interpretation of control design specifications in the frequency domain. Furthermore, it provides clear guidelines for the design of controllers so as to achieve robust performance in the presence of plant uncertainty.

The first step in the controller design procedure is the development of a synthesis model which can serve as an interface between the designer and the $\mathcal{H}_\infty$ controller synthesis algorithm. Consider the

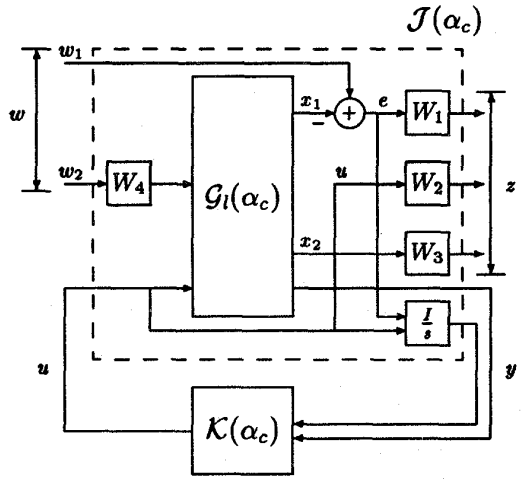

Figure 3.1: Synthesis model.

feedback system shown in figure 3.1, where $\mathcal{G}_l(\alpha_c)$ is obtained from the linearized model of the AUV and $\mathcal{K}(\alpha_c)$ is the controller to be designed. The correspondence between the standard notation of figure 3.1 [2] and that introduced in Section 2 for incremental variables will be clear form the context. The block $\mathcal{J}(\alpha_c)$ within the dashed line is the synthesis model, which is derived from the linearized model of the plant by appending the depicted weights. In practice, the weights serve as tuning "knobs" which the designer can adjust to meet the desired performance specifications.

The signal w_1 corresponds to the vector of input commands that must be tracked. In this design example, it includes linear positions. The signal w_2 represents the noise inputs to each of the sensors, and disturbance inputs to the states of the plant. The signal u corresponds to the control inputs to the system. The signal x_1 represents the components of the state vector that must track the input commands, while the vector x_2 contains the remaining state variables that must be weighed.

The outputs of W_1, W_2, and W_3 constitute the vector z. Since zero steady-state error in tracking the step command for all variables in x_1 was required, the weighting function W_1 was chosen as a diagonal of integrators. The integrator gains were adjusted to get desired command response bandwidths. The weights W_3, W_4 do not include any dynamics. In

order to drive $\delta_{a,c}$ to zero in steady state, an integrator was included in W_2.The signal y includes all the states of the plant $\mathcal{G}_l(\alpha_c)$, together with the appended integrator states that correspond to integrators.

Given a design model, suppose that the feedback system is well posed and let $\mathcal{T}_{zw}$ denote the closed loop transfer matrix from w to z. The $\mathcal{H}_\infty$ synthesis problem consists of finding, among all controllers that yield a stable closed loop system, a controller $\mathcal{K}(\alpha_c)$ that minimizes the maximum energy gain of the closed loop operator $\mathcal{T}_{zw}$, denoted $||\mathcal{T}_{zw}||_\infty$. This problem was solved using the methodology exposed in [8], see [11].

3.2 Non-linear Tracking Controller Implementation

A set of controllers was determined for a finite combination of values of $\mathbf{V}_T, \dot{\psi}$ and γ, and their parameters interpolated according to the scheduling vector α in a fixed bounded domain, see [11]. The implementation of the resulting non-linear gain scheduled controller was done by extending the D-methodology described in [7], which guarantees the following fundamental *linearization property*: the linearization of the nonlinear feedback control system about each equilibrium trajectory preserves the internal as well as the input-output properties of the corresponding linear closed loop designs.

Surprisingly, this property is often not satisfied by gain scheduled controllers proposed in the literature, see [7] and the references therein. In practice, violation of that property may lead to degradation in performance, or even instability, of the closed-loop system.

The D-methodology is based on the key observation that linear controllers are designed to operate on the perturbations of the plant's inputs and outputs about the equilibrium points. Proper blending of the different controllers requires that they have access to such perturbations, locally. This is achieved by differentiating some of the measured outputs before they are fedback to the gain scheduled controller. In order to preserve the input-output behaviour of the feedback system, integral action is provided at the input to the plant.

The gain scheduled controller implementation is depicted in figure 3.2, where $\mathcal{K}$ denotes the interpolation of the linear controllers obtained in Subsection 3.1. Notice that *the only external commands to the trajectory tracking controller are* $\mathbf{p}_C$ *and* $\dot{\psi}_C$, which are easily available from the trajectory generator.

It is important to stress that the D-method presented above requires differentiating some of the plant's measured outputs. Except for the case where some of the derivatives are available from dedicated sensors, this cannot be done in practice. In this case, the differentiation operator may simply replaced by a causal system with transfer function $\frac{s}{\tau s+1}$, or by a simple finite difference operator for discrete-time implementation, see [7]. It is also important to remark that the D-methodology would require that the time-

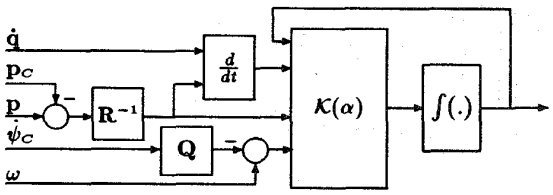

Figure 3.2: Tracking controller implementation

derivative of $\dot{\boldsymbol{\lambda}}_E$ be computed on-line. However, from the relations $\ddot{\mathbf{q}}_E = \ddot{\mathbf{q}}$ and $\dot{\boldsymbol{\lambda}}_E = \boldsymbol{\omega} - \mathbf{Q}\dot{\boldsymbol{\lambda}}_C$, it follows that the derivative is simply computed as depicted in figure 3.2. Thus, the method proposed avoids the need to feedforward trimming conditions for the state variables and inputs, except $\mathbf{p}_C$ and $\dot{\psi}_C$.

4 Simulation of Guidance and Control.

This section assesses the combined performance of guidance and control using dynamic models of the vehicle and its sensors suite. The reader is refered to [9] for the design of the multi-rate navigation system of the AUV MARIUS, and for a description of its navigation sensors. Measurements of linear position and velocity are provided by a Long Baseline (LBL) positioning system and a Doppler sonar, respectively.

In the simulations, the sensors for attitude estimation were sampled at 50 Hz, the Doppler sonar at 0.2 Hz, and the transponders were interrogated each second for linear position and velocity estimation and the integrated control and guidance systems were discretized at $10Hz$.

The reference for linear position in the $x-y$ plane is an $\mathcal{S}$ - shaped trajectory consisting of three straight lines $50m$ long each, and two semicircumferences with radii of $38m$. The reference trajectory in the vertical plane descends smoothly along the depth coordinate z with a slope of -10 deg. In order to simplify the interpretation of the simulation results, the trajectory was generated with a constant velocity $\mathbf{V}_T = 2.0m/s$.

The desired and observed trajectories are depicted in figure 4.1. The activity of some relevant state variables are condensed in figure 4.2. In this simulation, the LBL system uses four transponders located in positions $\{-40, 0, 160\}, \{130, 0, 150\}, \{-40, 190, 170\}$ and $\{140, 190, 135\}$, specified in meters.

At the beginning of the maneuver, the actuation variables are essentially constant during the first $25s$. Upon entering the circular path, the rudder deflects to create a torque that will impart the desired rotational speed to the vehicle. Once the desired speed is reached, the rudder deflects slightly in the opposite direction to stabilize the rotation. This maneuver is characteristic of vehicles that are unstable in yaw.

At the middle of the first turn, the vehicle shows a pronounced rotation in pitch in order to converge rapidly to the desired vertical inclination of -10 *deg*. This rotation is achieved by deflecting the common

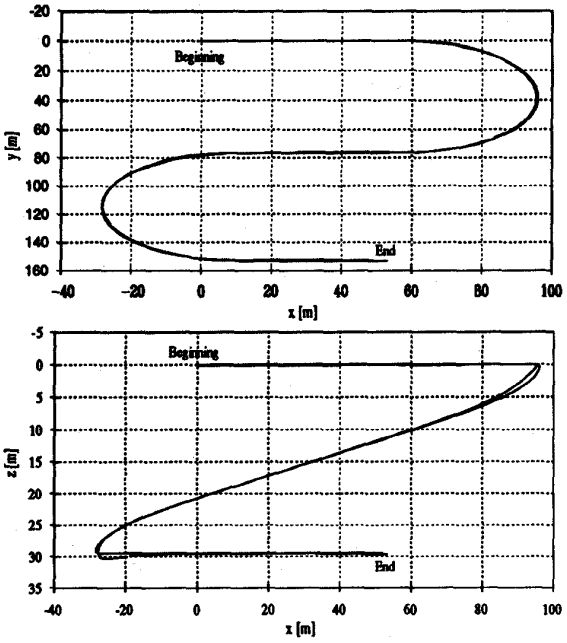

Figure 4.1: Reference and observed trajectory - horizontal and vertical planes.

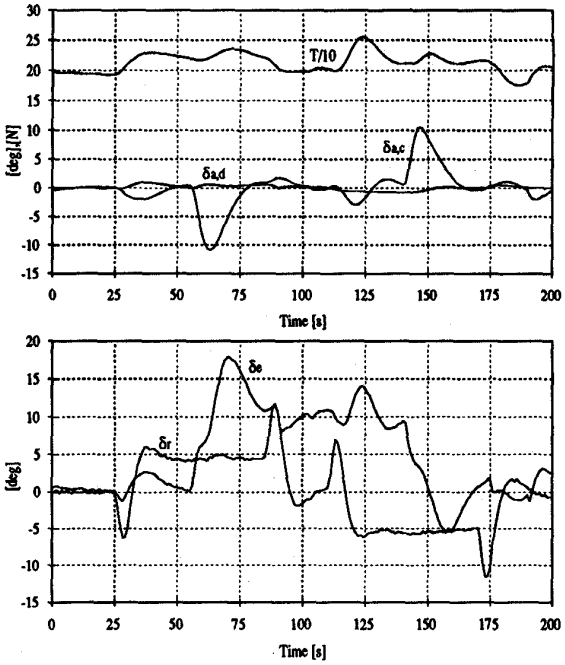

Figure 4.2: Control activity: Rudder (δ_r), Ailerons ($\delta_{a,c}$ and $\delta_{a,d}$), Elevator (δ_e) and Thruster (T).

aileron $\delta_{a,c}$ and the elevator δ_e in opposite directions, so as to generate a pure torque. When the vehicle reaches the desired orientation, $\delta_{a,c}$ and δ_e decrease. However, their values don't tend to zero, since they must counteract the restoring torque due to the combined effects of buoyancy and gravity.

When the vehicle reaches the end of the first turn, there is a strong deflection in the rudder to drive the velocity of rotation to zero. Similar comments apply to the remaining part of the trajectory.

It is important to remark that the thrust activity rises during maneuvers that require large deflection of the control surfaces. This is required to counteract the increase in drag, which tends to slow down the vehicle.

References

[1] M. Abkowitz, "Lectures on Ship Hydrodynamics - Steering and Maneuverability," *report No. Hy-5, Hydrodynamics Department*, Technical University of Denmark, Lyngby, Denmark, May 1964.

[2] J. C. Doyle, B. Francis and A. Tannenbaum, *Feedback Control Theory*, MacMillan Publishing Company, 1992.

[3] J. C. Doyle, K. Glover, P. P. Khargonekar, and B. A. Francis, "State space solutions to standard $\mathcal{H}_2$ and $\mathcal{H}_\infty$ control problems," *IEEE Transactions on Automatic Control*, AC- 34(8), August 1989,pp. 831–847.

[4] Elgersma,M. R., "Control of Nonlinear Systems Using Partial Dynamic Inversion" *Ph. D. Thesis*, University of Minnesota, Minneapolis, MI, 1988.

[5] D. Fryxell and A. Pascoal. "Modeling, Identification and Control of the AUV MARIUS," *SOUV-Technical Report*, Institute for Systems and Robotics,1994.

[6] A. Healey and D. Lienard, "Multivariable sliding mode control for autonomous diving and steering of unmanned underwater vehicles," *IEEE Journal of Oceanic Engineering*, Vol. 18, N0.3, July 1993, pp. 327-339.

[7] I. Kaminer, A. Pascoal, P. P. Khargonekar, and C. Thompson, "A Velocity Algorithm for the Implementation of Non-Linear Gain-Scheduled Controllers," Proc. 1993 European Control Conference, pp. 787-792. Full paper version accepted for publication in *Automatica*.

[8] P. Khargonekar, K. Poola and A. Tannenbaum, "Robust Control of Linear Time-Invariant Plants using Periodic Compensation," *IEEE Transactions on Automatic Control*, Vol. AC-30, pp.1088–1096, November 1985.

[9] P. Oliveira, A. Pascoal and C. Silvestre. "Guidelines for the Design of Advanced Navigation Systems for AUVs," *SOUV-Technical Report*, Institute for Systems and Robotics, 1994.

[10] A. Pascoal," The AUV MARIUS: Mission Scenarios, Vehicle Design, Construction and Testing," *Proceedings of the 2nd Workshop on Mobile Robots for Subsea Environments*, Monterey Bay Aquarium, Monterey, California, USA, May 1994.

[11] C. Silvestre, A. Pascoal and I. Kaminer. "Design of Integrated Guidance and Control Systems for AUVs" *SOUV-Technical Report*, Institute for Systems and Robotics, 1994.